

## Neutron Reflectivity of an Oil-Water Interface

L. T. Lee,<sup>(1)</sup> D. Langevin,<sup>(2)</sup> and B. Farnoux<sup>(1)</sup>

<sup>(1)</sup>Laboratoire Léon Brillouin, Centre d'Etudes Nucléaires de Saclay, Gif-sur-Yvette, France

<sup>(2)</sup>Laboratoire de Physique Statistique, Ecole Normale Supérieure, Paris, France  
(Received 17 June 1991)

We report for the first time a study of the specular reflectivity of neutrons by an oil-water interface. We have overcome the problem of neutron absorption in the upper oil phase by using thin oil layers of well controlled thickness. The study is performed on an oil-water interface covered by a surfactant layer previously studied by light scattering and ellipsometry. The neutron study allows us to determine the thickness of the surfactant layer and the oil-water interfacial roughness, which is large due to the ultralow interfacial tension.

PACS numbers: 68.10.Cr, 68.15.+e

Neutron reflectivity is a powerful technique for the investigation of interfacial structures (with a spatial resolution of a few angstroms). It has been successfully applied to the study at liquid-air interfaces of surfactant monolayers [1] and of polymer solutions [2]. Studies of solid-liquid interfaces have also been reported recently [3]. Because of the wide occurrence of liquid-liquid interfaces, it seems of importance to extend the method to this case, for which, to our knowledge, there has been no reported data. In this paper, we present, for the first time, results for an oil-water interface in the presence of a surfactant layer.

In principle, x-ray reflectivity allows one to obtain the same type of information on surface layers [4]. In practice, the two techniques are complementary because the contrast conditions are different. X-ray sources are more powerful and allow studies at angles further away from the critical angle than neutrons. But, with x rays, one cannot perform contrast variations by isotopic substitution. In the present study this is of importance, as will be discussed later.

In the study of a liquid-liquid interface, the neutron beam traverses an upper liquid phase. The absorption coefficient of neutrons is small for most materials (about  $0.14 \text{ cm}^{-1}$  for  $\text{D}_2\text{O}$  including pure absorption and incoherent scattering). But in reflectivity experiments, the grazing incidence angle  $\theta$  is of the order of milliradians, and the distance traveled by neutrons in the upper phase can be very large:  $d/\theta$  for a layer thickness  $d$ . In the present study, in order to limit the loss in intensity, we have kept the thickness of the upper oil phase to ultrathin dimensions.

Our aim is the structural characterization of surfactant layers at oil-water interfaces. We have studied these interfaces with optical techniques: surface light scattering to measure their interfacial tension and ellipsometry to measure their thickness [5]. In ellipsometry, one measures the ellipticity  $\rho$  of the light reflected at the Brewster angle, which contains contributions of the surfactant layer thickness  $d$  and of the oil-water roughness due to thermal fluctuations. In the case of monolayers producing low interfacial tension at the oil-water interface, the

roughness contribution to the ellipticity is dominant and is given by (in reduced units) [6] by

$$\eta_r = \frac{\lambda}{\pi} \frac{\varepsilon_1 - \varepsilon_2}{(\varepsilon_1 + \varepsilon_2)^{1/2}} \rho_r = -\frac{3k_B T}{8} \frac{(\varepsilon_1 - \varepsilon_2)^2}{\varepsilon_1 + \varepsilon_2} \frac{1}{\sqrt{K\gamma}}, \quad (1)$$

where  $\varepsilon_1$  and  $\varepsilon_2$  are the dielectric constants of the coexisting phases,  $\lambda$  the light wavelength,  $k_B$  the Boltzmann constant,  $T$  the absolute temperature,  $\gamma$  the interfacial tension, and  $K$  the modulus of bending elasticity of the monolayer.  $K$  controls the upper cutoff for the wave vectors of thermally excited capillary waves, the mean-square amplitude of which is given by

$$\begin{aligned} \langle \zeta^2 \rangle &= \frac{1}{2\pi} \int \frac{k_B T q dq}{(\rho_2 - \rho_1)g + \gamma q^2 + Kq^4} \\ &= \frac{k_B T}{4\pi\gamma} \ln \left[ \frac{\gamma^2}{(\rho_2 - \rho_1)gK} \right], \end{aligned} \quad (2)$$

the lower cutoff being controlled by gravity;  $\rho_1$  and  $\rho_2$  are the densities of the coexisting phases and  $g$  is the gravity constant.

The data reported in this paper deal with the water-octane interface in the presence of monodecyl tetraglycol ether ( $\text{C}_{10}\text{E}_4$ ). The interfacial tension varies significantly with temperature in the range  $17^\circ\text{C} < T < 34^\circ\text{C}$  (Fig. 1) [5]. When the measured ellipticity is plotted versus  $\gamma^{-1/2}$ , one obtains a straight line as predicted by Eq. (1). This allowed us to determine the bending elastic constant,  $K = 0.51 k_B T$  [5]. The remaining contributions to the ellipticity can be extracted from the intercept of the line of Fig. 1 at the origin (limit of large  $\gamma$ ), which is  $\eta = -0.045 \text{ \AA}^{-1}$ . Assuming this to be the contribution of the monolayer thickness, given by Drude's formula  $\eta = d(\varepsilon - \varepsilon_1)(\varepsilon - \varepsilon_2)/\varepsilon$  [7], where  $\varepsilon$  is the surfactant dielectric constant, one gets a negative thickness:  $d = -1.9 \text{ \AA}$ . Clearly there is an inconsistency here, probably due to a contribution of optical anisotropy as observed in other monolayers [8]. Neutron reflectivity, on the other hand, is not affected by anisotropy in the surface layer.

The neutron reflectivity experiments were conducted on

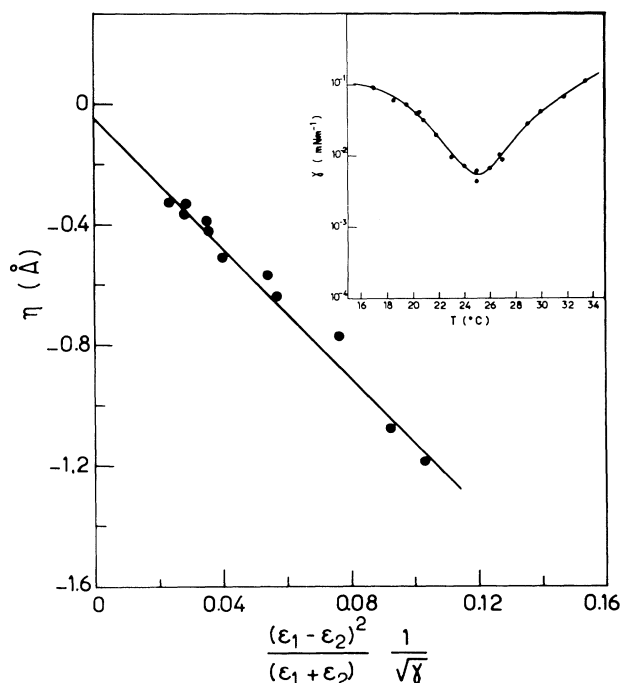


FIG. 1. Reduced ellipticity of the light reflected by the interface between octane and water in the presence of  $C_{10}E_4$  at different temperatures vs the corresponding reduced interfacial tensions. Inset: Interfacial tension vs temperature for the same system. Data from Ref. [5].

a prototype time-of-flight reflectometer DESIR in the Orphee reactor. A detailed description of the reflectometer has been given elsewhere [9]. The neutron wavelengths range from 3 to 15 Å and the incident angle is about  $1.0^\circ$ . The angular resolution of the spectrometer ( $\sim 5\%$ ) is determined using high-purity solvents the refractive indices of which are known.

The aluminum sample container ( $100 \times 30 \times 1$  mm) is enclosed in a first cell with quartz windows to minimize evaporation of the liquids. This first cell is equipped with a thermocouple to control the sample temperature. This ensemble is then enclosed in a second cell which helps maintain the temperature of the air surrounding the first cell constant. Such careful control is necessary to reduce

$$r = \frac{r_{01} + r_{12} \exp(2i\Phi) + r_{23} \exp[2i(\Phi + \varphi)] + r_{01}r_{12}r_{23} \exp(2i\varphi)}{1 + r_{01}r_{12} \exp(2i\Phi) + r_{12}r_{23} \exp(2i\varphi) + r_{01}r_{23} \exp[2i(\Phi + \varphi)]}, \quad (3)$$

where

$$r_{ij} = \frac{n_i \sin \theta_i - n_j \sin \theta_j}{n_i \sin \theta_i + n_j \sin \theta_j},$$

$\theta_i$  being the angle of incidence of the neutron beam with the surface in medium  $i$ , and  $n_i$  the neutron refractive index in medium  $i$ . The media are air ( $i=0$ ), oil ( $i=1$ ), surfactant ( $i=2$ ), and water ( $i=3$ ). The phase shifts are  $\Phi = q_z D = 2\pi \sin \theta_1 n_1 D / \lambda$  and  $\varphi = q_z d = 2\pi \sin \theta_2 n_2 d /$

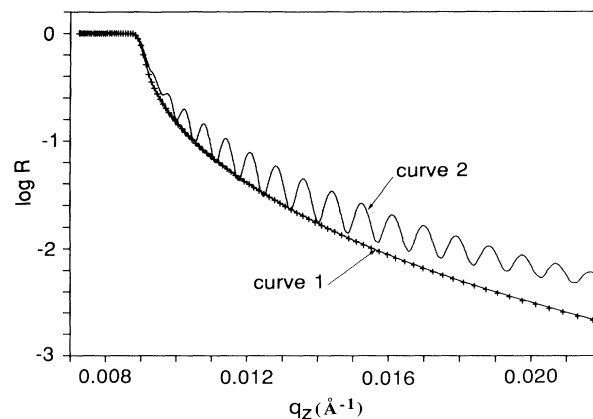


FIG. 2. Calculated neutron reflectivity curves of a thin film of deuterated octane ( $D=2970$  Å) on deuterated water (curve 1); deuterated octane on deuterated water in the presence of protonated  $C_{10}E_4$  using  $D=2970$  Å,  $d=20$  Å, and  $\phi_s=0.8$  (curve 2); and protonated  $C_{10}E_4$  ( $d=20$  Å,  $\phi_s=0.8$ ) on deuterated water in the absence of deuterated octane (crosses). For all three curves, Eq. (3) was used and  $\langle \zeta^2 \rangle = 0$ .

condensation of the liquid sample on the cell windows and, more importantly for this experiment, to minimize the variation of the thickness of the oil layer during data acquisition. The temperature was kept constant at  $17^\circ\text{C}$ . The acquisition time was 3 h.

After testing several different contrast conditions, we have chosen deuterated oil and water, keeping the surfactant protonated. When no surfactant is added, the reflectivity is only from the top oil surface since both the deuterated oil and water have the same scattering length density (Fig. 2, curve 1). When a protonated surfactant layer is present, the reflectivity curve exhibits oscillations (Fig. 2, curve 2) due to interferences between the beams reflected at the oil-air, oil-surfactant, and surfactant-water interfaces. The hypothetical case where the surfactant layer is present but the octane is absent is also given in Fig. 2 (crosses). Therefore, using this isotopic composition, the oscillations are attributed solely and unambiguously to the presence of the protonated surfactant layer sandwiched between the deuterated octane and deuterated water. Indeed, the reflectance is given by [10]

$\lambda$ , where  $D$  and  $d$  are the thicknesses of the oil and surfactant layers, respectively, and  $q_z$ , the normal component of the incident neutron wave vector. To a first approximation,  $r_{12} = -r_{23} \ll r_{01}$  and the reflectivity takes the simple form

$$R = |r|^2 \approx \frac{r_{01}^2 + 4r_{01}r_{12} \sin \varphi \sin(2\Phi + \varphi)}{1 + 4r_{01}r_{12} \sin \varphi \sin(2\Phi + \varphi)}, \quad (4)$$

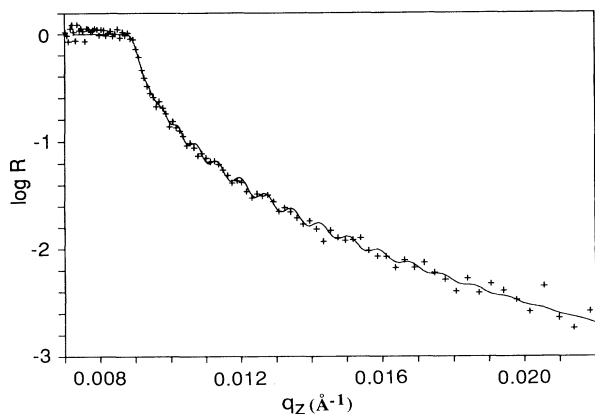


FIG. 3. Experimental data of neutron reflectivity of deuterated octane-protonated  $C_{10}E_4$  deuterated water system at  $17^\circ\text{C}$  (crosses). Calculated curve uses Eq. (3) and  $D=2970 \text{ \AA}$ ,  $d=20 \text{ \AA}$ ,  $\phi_s=0.8$ ,  $\langle\zeta^2\rangle^{1/2}=90 \text{ \AA}$  as explained in the text (solid curve).

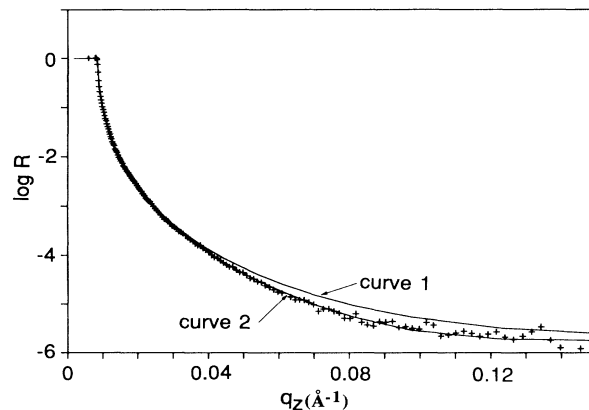


FIG. 4. Experimental data of neutron reflectivity from the free surface of deuterated toluene (crosses); calculated reflectivity curve with  $\langle\zeta^2\rangle=0$  (curve 1); calculated reflectivity curve with  $\langle\zeta^2\rangle^{1/2}=5 \text{ \AA}$  (curve 2).

which shows that the oscillations are mainly due to the variations of  $\Phi$ . The theoretical curve calculated with Eq. (3) is shown in Fig. 2, curve 2.

The oscillations observed experimentally have a smaller amplitude (Fig. 3, crosses). For the range of wave vectors studied in the present experiment, the roughness of the oil surface has no influence on the data (see Fig. 4 and below). But the roughness of the oil-water interface is large due to its low interfacial tension. In order to account for this roughness of magnitude  $\langle\zeta^2\rangle^{1/2}$ ,  $r_{12}$  has to be multiplied by  $\exp(-q_z^2\langle\zeta^2\rangle)$  [11]. The experimental curve compares well with the theoretical curve (Fig. 3, solid line) calculated by taking  $D=2970 \text{ \AA}$ ,  $d=20 \text{ \AA}$ , and  $\phi_s=0.8$ , where  $\phi_s$  is the volume fraction of surfactant in the monolayer region (this means that there is 20% water and octane in this region). The periodicity of the oscillations depends mainly on  $D$ , the determination of which is very accurate:  $2970 \pm 20 \text{ \AA}$ . The accuracies on  $d$  and  $\phi_s$  are, on the other hand, comparatively not as good. Equally good fits are obtained with  $d=16 \text{ \AA}$  and  $\phi_s=1$  or  $d=30 \text{ \AA}$  and  $\phi_s=0.54$ , because the reflectivity is only sensitive to the product  $d\phi_s$ . But the couple  $d=20 \text{ \AA}$  and  $\phi_s=0.8$  is the most probable: Indeed, the thickness  $20 \text{ \AA}$  compares well with the length of the surfactant molecule [12], and the surfactant concentration (80%) in the monolayer is such that it allows for some degree of oil and water penetration into the layer, as is commonly the case in these very flexible surfactant layers [13]. The fit also incorporates a roughness of  $\langle\zeta^2\rangle^{1/2}=90 \text{ \AA}$  for the monolayer. The roughness therefore reduces the amplitude of the oscillations as compared with curve 2 in Fig. 2 where roughness is ignored. The value of the roughness used to fit the data in Fig. 3 is calculated from Eq. (2) with  $\gamma=0.08 \text{ dyn/cm}$ , the interfacial tension at  $17^\circ\text{C}$ . At higher temperatures, the roughness is larger and the oscillations are completely smoothed out.

Let us note that  $\langle\zeta^2\rangle^{1/2}$  varies mainly as  $\gamma^{-1/2}$ . For the free surface of pure water ( $\gamma=72 \text{ dyn/cm}$ ), x-ray reflectivity and scattering data give  $\langle\zeta^2\rangle^{1/2} \approx 3 \text{ \AA}$  [14]. Comparing our data with these values, the ratio of the amplitudes of surface roughness is 30, and the ratio of interfacial tensions is 900, as expected. It has been reported recently that the amplitude of the roughness for the surface of ethanol is  $6.9 \text{ \AA}$  [15], whereas  $\gamma=22 \text{ dyn/cm}$ ; one would have expected to find  $\langle\zeta^2\rangle^{1/2} \approx 5.4 \text{ \AA}$ . But our neutron reflectivity data obtained on CRISP at the Rutherford Appleton Laboratory on the free surface of toluene ( $\gamma=28.5 \text{ dyn/cm}$ ) give  $\langle\zeta^2\rangle^{1/2}=5 \text{ \AA}$  (Fig. 4) in good agreement with expectations. We can thus reasonably conclude that in our case, the measured roughness of the oil-water interface in the presence of the surfactant layer is correct.

In conclusion, we have measured both the thickness and the roughness of a surfactant layer at an oil-water interface. The accuracy on the oil thickness is better although this is not of direct interest for the experiment. The measured thickness of the surfactant layer is an equivalent thickness,  $d\phi_s=16 \text{ \AA}$ , because the surfactant concentration in the layer  $\phi_s$  cannot be determined accurately. Reasonable expectations are  $d=20 \text{ \AA}$  and  $\phi_s=0.8$ . The roughness of the surfactant layer,  $90 \text{ \AA}$ , is much larger than its thickness, and is in excellent agreement with the theoretical predictions for thermally excited surface waves. These preliminary results open a large and promising field of investigation on the liquid-liquid interfaces.

[1] J. Penfold and R. K. Thomas, *J. Phys. Condens. Matter* **2**, 1369 (1990).

[2] X. Sun, E. Bouchaud, A. Lapp, B. Farnoux, M. Daoud, and G. Jannink, *Europhys. Lett.* **6**, 207 (1988); A. R.

- Rennie, R. J. Crawford, E. M. Lee, R. K. Thomas, T. L. Crowley, S. Roberts, M. S. Qureshi, and R. W. Richards, *Macromolecules* **22**, 3466 (1989); L. T. Lee, O. Guiselin, B. Farnoux, and A. Lapp, *Macromolecules* **24**, 2518 (1991).
- [3] E. M. Lee, R. K. Thomas, P. G. Cummins, E. J. Staples, J. Penfold, and A. R. Rennie, *Chem. Phys. Lett.* **162**, 196 (1989); S. K. Satija, C. F. Majkrzak, T. P. Russell, S. K. Sinha, E. B. Sirota, and G. J. Huges, *Macromolecules* **23**, 3860 (1990); T. Cosgrove, T. G. Heath, J. S. Phipps, and R. M. Richardson, *Macromolecules* **24**, 94 (1991).
- [4] P. S. Pershan, *Faraday Discuss. Chem. Soc.* **89**, 231 (1990).
- [5] L. T. Lee, D. Langevin, J. Meunier, K. Wong, and B. Cabane, *Prog. Colloid. Polym. Sci.* **81**, 209 (1990).
- [6] J. Meunier, *J. Phys. (Paris), Lett.* **46**, L1005 (1985).
- [7] P. Drude, *Ann. Phys. (Paris)* **43**, 126 (1891).
- [8] H. Bercegol, F. Gallet, J. Meunier, and D. Langevin, *J. Phys. (Paris)* **50**, 2277 (1989).
- [9] B. Farnoux, Laboratoire Léon Brillouin, CEA, Activity Report, 1987-1988 (unpublished).
- [10] O. S. Heavens, *Optical Properties of Thin Solid Films* (Dover, New York, 1965).
- [11] P. Beckman and A. Spizzichino, *The Scattering of Electromagnetic Radiation from Rough Surfaces* (Pergamon, New York, 1963); L. Nevot and P. Croce, *Rev. Phys. Appl.* **15**, 761 (1980).
- [12] C. Tanford, *The Hydrophobic Effect* (Wiley, New York, 1973).
- [13] A. M. Cazabat, D. Chatenay, D. Langevin, and J. Meunier, *Faraday Discuss. Chem. Soc.* **76**, 291 (1983).
- [14] D. K. Schwartz, M. L. Schlossman, E. H. Kawamoto, G. J. Kellogg, P. S. Pershan, and B. M. Ocko, *Phys. Rev. A* **41**, 5687 (1990).
- [15] M. K. Sanyal, S. K. Sinha, K. G. Huang, and B. M. Ocko, *Phys. Rev. Lett.* **66**, 628 (1991).